Received: 3 March 2021 | Revised: 15 January 2022 | Accepted: 19 January 2022

DOI: 10.1002/nbm.4703

RESEARCH ARTICLE

NMR IN BIOMEDICINE WILEY

Perfusion system for studying dynamic metabolomics in rat brain slices exposed to oxygen–glucose deprivation using proton and phosphorus nuclear magnetic resonance

Alicja Molska[1,2] | Deborah K. Hill[1] | Trygve Andreassen[1] | Marius Widerøe[1]

[1]Department of Circulation and Medical Imaging, Faculty of Medicine and Health Sciences, Norwegian University of Science and Technology (NTNU), Trondheim, Norway

[2]Department of Biotechnology and Nanomedicine, SINTEF Industry, Trondheim, Norway

Correspondence
Marius Widerøe, Department of Circulation and Medical Imaging, Faculty of Medicine and Health Sciences, NTNU, Medisinsk teknisk forskningssenter (MTFS), Post box 8905, 7491 Trondheim, Norway.
Email: marius.wideroe@ntnu.no

Funding information

Norwegian University of Science and Technology, Faculty of Medicine and Health Sciences (AM: PhD stipend).

The aim of the current study was to establish a controlled and reproducible model to study metabolic changes during oxygen–glucose deprivation (OGD) in rat brain using a nuclear magnetic resonance (NMR)-compatible perfusion system. Rat brains were cut into 400-μm thick slices and perfused with artificial cerebrospinal fluid (aCSF) in a 10-mm NMR tube inside a 600-MHz NMR spectrometer. Four experimental conditions were tested: (1) continuous perfusion with aCSF with glucose and normoxia, and (2) 30-, (3) 60-, or (4) 120-min periods of OGD followed by reperfusion of aCSF containing glucose and normoxia. The energetic state of perfused brain slices was measured using phosphorus (^{31}P) NMR and metabolite changes were measured using proton (^{1}H) NMR. aCSF samples were collected every 30 min and analyzed using ^{1}H NMR. The sample temperature was maintained at 36.7 ± 0.1°C and was checked periodically throughout the experiments. Brain slice histology was compared before and after OGD in the perfusion system using hematoxylin–eosin–saffron staining. NMR data clearly distinguished three severity groups (mild, moderate, and severe) after 30, 60, and 120 min of OGD, respectively, compared with the control group. ^{31}P NMR spectra obtained from controls showed that phosphocreatine levels were stable for 5 h inside the perfusion system. Control ^{1}H NMR spectra showed that lactate, N-acetylaspartic acid, glutamate, γ-aminobutyric acid, and creatine metabolite levels were stable over time, with lactate levels having a tendency to gradually increase due to the recirculation of the aCSF in the perfusion system. A controlled and reproducible perfusion system was established to study the energetic and metabolic changes in rat brain slices during and after OGD of varying severity.

KEYWORDS
^{1}H NMR, ^{31}P NMR, hypoxic–ischemic brain injury, oxygen–glucose deprivation, perfusion system, rat brain slices

Abbreviations used: 1D, one-dimensional; ^{1}H NMR, proton nuclear magnetic resonance; ^{31}P NMR, phosphorus nuclear magnetic resonance; aCSF, artificial cerebrospinal fluid; ATP, adenosine triphosphate; Cr, creatine; DSS, sodium trimethylsilylpropanesulfonate; GABA, γ-aminobutyric acid; Glu, glutamate; GPC, glycerylphosphorylcholine; HES, hematoxylin–erythrosine–saffron; HI, hypoxia–ischemia; Lac, lactate; NAA, N-acetylaspartic acid; OGD, oxygen–glucose deprivation; Pi, inorganic phosphate; PCr, phosphocreatine; RG, receiver gain.

1 | INTRODUCTION

Brain injury resulting from insufficient blood and oxygen supply to the brain can cause long-term neurological disabilities and death in all age groups. Neonatal hypoxia–ischemia (HI), cardiac arrest, and stroke are the diseases most frequently associated with this condition.[1] Although current clinical practice with hypothermia treatment of neonatal HI and cardiac arrest, and rapid clot removal in stroke have reduced mortality and neurological sequela,[2] there is still a need for better understanding of the pathophysiological mechanisms and for new neuroprotective treatments.

The pathophysiology underlying hypoxic and ischemic brain injuries is initiated by a lack of oxygen that forces the cells to switch from aerobic to anaerobic metabolism. This limits the cells' ability to produce high energy substrates (primarily adenosine triphosphate [ATP]) as the yield from anaerobic glucose metabolism is only about 1/19th of that from aerobic metabolism. Anaerobic metabolism also results in accumulation of lactate (Lac) as the end "waste" product of glycolysis, making the cells acidic.[3] In addition, glucose levels in tissues become low due to a lack of or limited blood supply; anaerobic metabolism also comes to a halt, resulting in energy failure of the cells. As most cellular processes are dependent on high energy substrates, the failure to produce them results in several events that can lead to cellular death: an inability to maintain membrane potential, excitotoxicity due to reduced reuptake of glutamate (Glu) from synapses, initiation of apoptotic cascades, initiation of inflammatory processes, and necrosis.[4]

Model systems are needed to study pathophysiological mechanisms and new strategies for neuroprotection. Multiple in vivo animal models exist, but are often hampered by high variability in injury severity depending on procedural aspects, animal strains, body weight, and environmental factors such as the influence of temperature and feeding that are hard to control.[5] Differences in pharmacokinetics and persistence of the blood–brain-barrier also complicate the use of animal models for initial testing of neuroprotective strategies. On the other hand, in vitro and ex vivo models permit a more reproducible and direct modulation of the brain cells. The most widely used in vitro and ex vivo model of ischemic injury is the oxygen–glucose deprivation (OGD) model.[6] Even although in vitro cell cultures offer simplified, high throughput systems to study diseases, drug effects, and changes to biological processes by controlling environmental factors, they lack important intracellular interactions and consequently poorly mimic the in vivo situation. To establish a more relevant OGD model that better reflects the complexities of the brain injury environment, an ex vivo brain tissue slice model is preferred. In this model, brain slices are perfused with artificial cerebrospinal fluid (aCSF) and this allows control over temperature, nutrients, and oxygen supply to mimic physiological and pathophysiological conditions.[7,8] The brain slices retain the tissue architecture of the brain regions that they originated from and maintain neuronal activities.[9] Such a model offers several advantages over in vivo models, for example, immediate and direct access to the extracellular compartment due to the lack of a blood–brain barrier and direct control over environmental factors.[10] In addition, a highly reproducible ex vivo model has the potential to reduce the number of animals needed per experiment compared with in vivo models, in line with the animal research principles of the three Rs (i.e., replacement, reduction, and refinement).[11]

Phosphorus (^{31}P) and proton (^{1}H) nuclear magnetic resonance (NMR) are valuable tools with which to study energy metabolism. Because NMR is noninvasive, measurements can be performed on living cells, tissue, animals, or humans without influencing the homeostasis and ongoing processes. NMR thus also provides the valuable possibility to study real-time changes in energy metabolism caused by hypoxia and ischemia, and how it is modulated by different neuroprotective strategies.[12]

The aim of this study was to design an NMR-compatible perfusion system that allows dynamic metabolic measurements of rat brain slices under normal conditions and under conditions mimicking brain HI, providing the opportunity to learn more about the pathophysiology, and possible effects of treatments. Special emphasis was placed on creating a system able to maintain and monitor physiological temperature in the sample, a significant factor in HI brain injury.

2 | METHODS

2.1 | Materials

Deuterium oxide (D_2O) (99.9% atom % D), Phenol Red Solution 0.5%, KCl, d-(+)-glucose, $NaHCO_3$, $MgCl_2$, NaH_2PO_4, $CaCl_2$, and glass beads (Ø = 1 mm, SKU: Z250473) were obtained from Sigma-Aldrich Chemie GmbH (Germany). NaCl and sucrose were purchased from Fluka Analytical, while sodium trimethylsilylpropanesulfonate (DSS) was obtained from Chem Cruz. Gas bottles of 95% O_2/5% CO_2 and 95% N_2/5% CO_2 were purchased from AGA (Norway). The perfusion system in-line tubing (polyethylene, inside diameter [ID] = 1.40 mm, outside diameter [OD] = 1.90 mm) and primary out-line tubing (silastic, ID = 1.57 mm, OD = 2.41 mm) were obtained from Fisher. The silicon secondary out-line tubing (ID = 1.50 mm, OD = 2.41 mm) was purchased from ROTH, and the silicon water-heated tube (ID = 10.0 mm, OD = 14.0 mm) was purchased from VWR. Custom-made adapters used to connect in- and out-line tubing inside the water-heated tube were made of stainless steel and polymethylmethacrylate.

2.2 | Animals

Sprague Dawley rats (*Rattus norvegicus*) were obtained from Elevage Janvier (Le Genest Saint Isle, Laval, France). Their sex, age, and body weight assigned to different experimental groups is shown in Table 1. All animal experiments were performed according to the European Union and Norwegian regulations and guidelines for animal experimentation, and were approved by the Norwegian authority on animal welfare (Mattilsynet, FOTS 10105). Rats were housed in groups of three in a controlled light/dark cycle (12 h/12 h), temperature at 21–22°C, humidity at 50%–55%, with environmental enrichment, food, and water ad libitum.

2.3 | Brain slices and perfusion system

Animals were anesthetized with 3%–4% isoflurane in a mixture of air (2.0 L/s) and O_2 (0.5 L/s). When a negative pedal pain reflex was obtained, the animal was decapitated using a guillotine. The whole brain was extracted from the skull and placed in ice-cold slicing aCSF containing 87 mM NaCl, 2.5 mM KCl, 25 mM d-(+)-glucose, 25 mM $NaHCO_3$, 3 mM $MgCl_2$, 1.25 mM NaH_2PO_4, 0.5 mM $CaCl_2$, 75 mM sucrose, and 0.1% (v/v) Phenol Red Solution in sterile H_2O. The slicing medium was prebubbled with 95% O_2/5% CO_2 gas mixture at a flow rate of 0.5 L/min for 30 min prior to the experiment. Next, brain slices were prepared according to the modified method in the protocol reported by Opitz-Araya and Barria.[13] The brain was cut into two hemispheres; one hemisphere was placed on the dissecting table, midline facing down, and the cerebellum was mounted on the cutting surface using glue. Then the cerebrum was cut into 400-μm thick slices, while the other hemisphere was formalin-fixed for further histological analysis. Intact brain slices (n = 20) from the cerebrum were selected and loaded into a 10-mm NMR tube containing 0.6 g of glass beads (Ø = 1 mm) and a sponge filter was placed above the tissue to keep slices in the NMR active region (Figure 1). The perfusion system supplied the NMR tube with 95% O_2/5% CO_2 prebubbled normal aCSF containing 124 mM NaCl, 2.5 mM KCl, 10 mM d-(+)-glucose, 26 mM $NaHCO_3$, 2 mM $MgCl_2$, 1.25 mM NaH_2PO_4, 2 mM $CaCl_2$, and 0.01% of DSS (w/w %) in water (90/10 v/v sterile/D_2O). The medium was dumped for the first 10 min to remove the remaining slicing aCSF medium and then the perfusing medium was recirculated until the start of the OGD period.

A 250-ml reservoir of normal aCSF and a 250-ml reservoir of OGD aCSF were placed in a water bath (40°C) outside the NMR spectrometer. The OGD aCSF contained 129 mM NaCl, 2.5 mM KCl, 26 mM $NaHCO_3$, 2 mM $MgCl_2$, 1.25 mM NaH_2PO_4, 2 mM $CaCl_2$, and 0.01% of DSS (w/w %) in water (90/10 v/v sterile/D_2O). The pH of all aCSF media (slicing, normal, and OGD) were adjusted to 7.4, and the media were filtered using

TABLE 1 Animal distribution in experimental groups: the control group, where the tissue was perfused in physiological medium and gases; the oxygen–glucose deprivation (OGD)-30, -60, and -120 groups, where the tissue was introduced with mild, moderate, and severe durations of OGD, respectively

Group	N	Sex	Age (weeks)	Body weight range (g)
Control	6	5 ♀, 1 ♂	11–39	276–471
OGD-30	5	5 ♀	10–12	358–472
OGD-60	6	6 ♀	10–11	384–531
OGD-120	5	4 ♀, 1 ♂	10–12	272–507

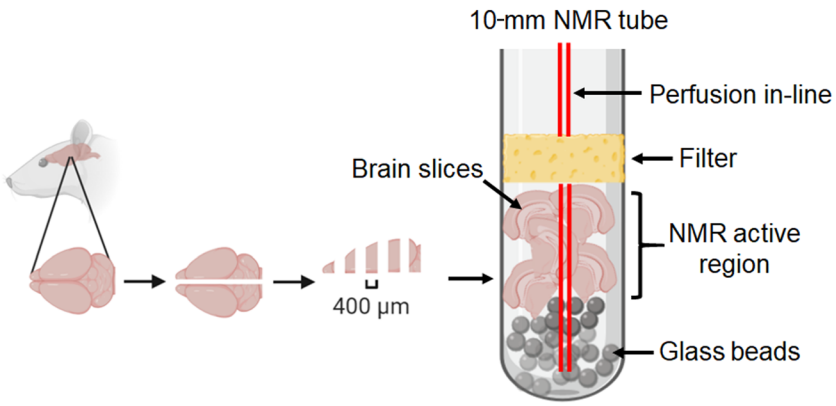

FIGURE 1 Illustration of the rat brain-slicing procedure and arrangement in the 10-mm NMR tube

a 0.22-μm filter. The medium (flow rate of 5 ml/min) was delivered to the NMR tube with brain slices via medical grade extension tubes pumped in a closed circuit with a peristaltic pump (Gilson, Minipuls 3, USA) while continuously bubbled with either 95% O_2/5% CO_2 carbogen mixture or 95% N_2/5% CO_2 gas (AGA) at a flow rate of 0.5 L/min (Figure 2).

2.4 | Temperature stability

To keep the perfused aCSF in the perfusion system at physiological temperature, the in-line and primary out-line were run through a 1.5-m long water-heated tube situated between the pump and the spectrometer bore (Figure 2). The heat bath (GD-120, VWR) for the water-heated tube was set to 60°C and its integrated pump allowed for continuous circulation of water throughout the heating line.

The temperature inside the spectrometer bore is measured by a temperature sensor located close to the NMR tube. This temperature, referred to in this article as "probe temperature", is kept stable by a combination of cold air and heating elements, but does not necessarily reflect the true temperature inside the NMR tube. Chemical shifts of labile proton nuclei, in water or hydroxy groups, are highly dependent on temperature and provide a way with which to measure the actual temperature in the active region. This has been utilized in previously reported in vivo NMR experiments, for example, from ^{1}H NMR frequency distances between H_2O and N-acetylaspartic acid (NAA) in pig brains.[14] In our work, DSS was added to the aCSF solution to provide a reference peak for calibration and normalization. The H_2O – DSS ^{1}H NMR frequency difference also proved valuable for measuring the temperature in the NMR tube. During the experiment, the temperature of the perfused aCSF sample in the spectrometer bore was measured after each ^{31}P NMR experiment using a ^{1}H NMR protocol (number of scans [ns] = 1, receiver gain [RG] = 1.6). The temperature measurement (scan and calculation) took approximately 1 min.

Standard temperature calibration of a pure nonperfused MeOH-d_4 sample in the NMR spectrometer bore with the probe temperature set to 310, 311, and 312 K was first performed using the method described by Findeisen et al.[15] Switching to a nonperfused aCSF sample, and keeping the other conditions unchanged, the distance between the H_2O and DSS peaks (set to 0 ppm) was measured at the three different probe temperatures after 20 min of temperature equilibration (Table 2).

The relationship between the difference in H_2O-peak and DSS-peak and the nonperfused aCSF sample temperature was linear (Figure 3), and the following equation to calculate the temperature (T) of a perfused aCSF sample in the spectrometer bore was derived: $T = \frac{\Delta(H_2O - DSS) \times 1000 - 7802.4}{-10.169}$, where $\Delta(H_2O - DSS)$ is the chemical shift difference between the H_2O and DSS peaks (ppm).

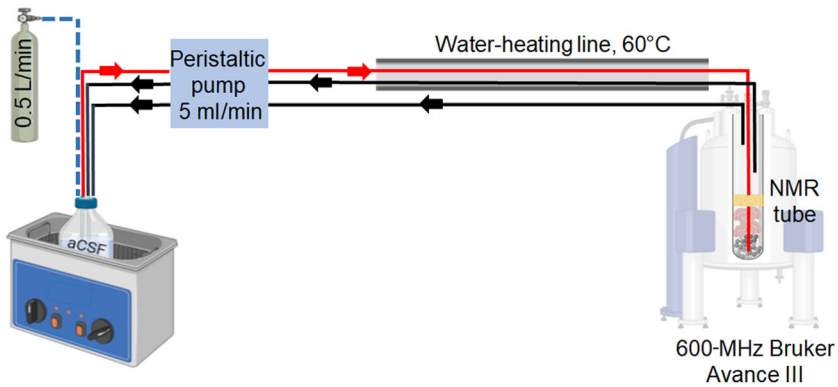

FIGURE 2 Illustration of the perfusion system for maintaining rat brain slices while placed in the NMR spectrometer bore. The perfusion system tubing consisted of in-line tubing (red) to deliver normal artificial cerebrospinal fluid (aCSF) to the brain slices located in the NMR tube inside the spectrometer bore; primary out-line tubing (black) was used to return the normal aCSF from the brain slices back to the normal aCSF reservoir and a secondary out-line (black) was placed in case of malfunction of the primary out-line. The in-line and primary out-line were placed inside a water-heated tube (60°C) between the pump and NMR spectrometer bore

TABLE 2 Differences between the H_2O peak and sodium trimethylsilylpropanesulfonate (DSS) peak in the nonperfused normal artificial cerebrospinal fluid sample at different probe temperatures

No.	Probe temp. (K)	Sample temp. (K)	ΔH_2O – DSS peak (ppm) * 1000
1	310	308.9	4.661
2	311	309.8	4.652
3	312	310.7	4.643

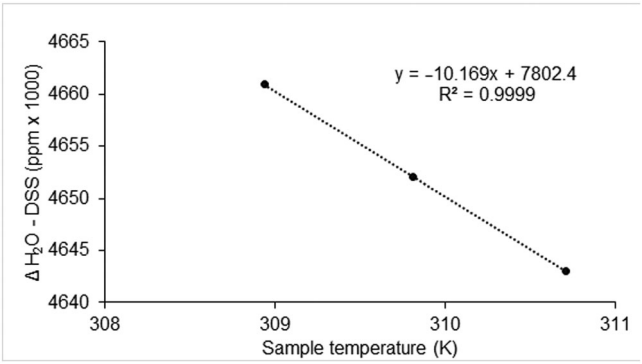

FIGURE 3 Calibration of sample temperature using the chemical shift difference between the H_2O peak and sodium trimethylsilylpropanesulfonate (DSS) peak as a function of sample temperature measured in the nonperfused normal artificial cerebrospinal fluid sample

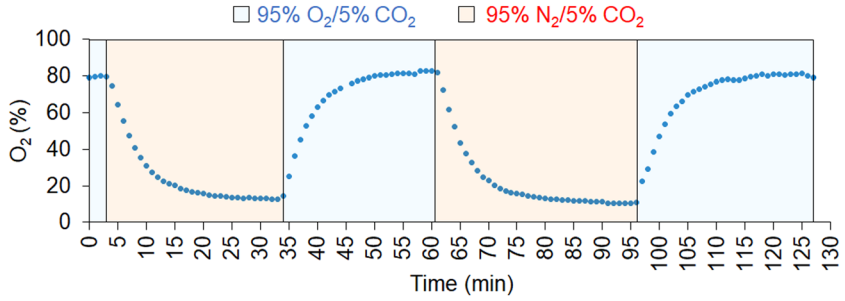

FIGURE 4 Oxygen levels of a perfused normal artificial cerebrospinal fluid sample outside the spectrometer bore continuously bubbled with 95% O_2/5% CO_2 or 95% N_2% CO_2 in the perfusion system over time

By knowing the distance between the chemical shift of the H_2O and DSS peaks ($\Delta = 4.652$ ppm) at the probe temperature set at 311 K in the nonperfused aCSF sample, the corresponding probe temperature of the perfused aCSF sample could be found. After increasing the probe temperature to 325 K, the same distance between the chemical shift of the H_2O and DSS peaks of a perfused aCSF sample was achieved ($\Delta = 4.652$ ppm). At the beginning of each experiment, the temperature of the probe in the spectrometer bore was adjusted based on the temperature of the perfused aCSF sample to reach 37 ± 1°C.

2.5 | Oxygenation of the aCSF sample

Oxygen levels were measured in the normal aCSF sample using the ISO-OXY-2 macrosensor (WPI, USA). The calibration curve was made according to the manufacturer's instructions. Then the oxygen level was measured from the normal aCSF sample set in the perfusion system with the flow rate at 5 ml/min outside the NMR spectrometer bore. The normal aCSF reservoir was placed in a water bath set at 37°C, and bubbled with either 95% O_2/5% CO_2 or 95% N_2/5% CO_2 gases for around 30 min. The time between achieving the minimum and maximum levels of oxygen in the buffer was measured.

The amount of O_2 in the perfused aCSF sample was measured at 37°C outside the spectrometer bore over a time period of more than 2 h. It took around 25 min to fully oxygenate or deoxygenate the aCSF (Figure 4). This result was used to design the OGD experiments, where both normal and OGD aCSF were prebubbled with either 95% O_2/5% CO_2 or 95% N_2/5% CO_2 for a minimum of 30 min prior to its incorporation into the perfusion system.

2.6 | Study design

Brain slices were perfused for at least 30 min with normal aCSF (95% O_2/5% CO_2) to let the set-up stabilize (normoxia). After achieving a stable sample temperature, ^{1}H NMR and 30-min ^{31}P NMR spectra were recorded. Control group samples were perfused with normal aCSF

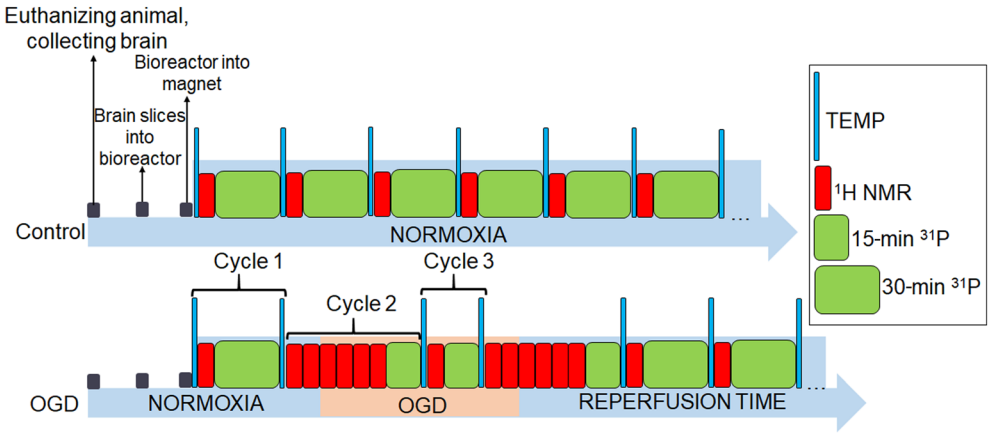

FIGURE 5 Study design of NMR experiments in the control and oxygen–glucose deprivation (OGD) groups starting from euthanizing the animal. The OGD time depends on the OGD group and lasts either 30, 60, or 120 min. Length of NMR experiments: TEMP = 11 s; ^{1}H NMR = 2 min 22 s or 120 s; ^{31}P NMR = 15 min 17 s or 30 min 22 s

(continuously bubbled with 95% O_2/5% CO_2), which was recirculated for the entire experiment. The cycle of TEMP - ^{1}H NMR - 30 min ^{31}P NMR - TEMP (cycle 1 in Figure 5) was continued for around 5 h from the time when the perfusion system was inserted into the magnet (Figure 5).

In the OGD experiments, after cycle 1 (Figure 5) with the normal aCSF medium, a single ^{1}H NMR experiment was conducted to confirm sample integrity, followed by a stacked series of five ^{1}H NMR experiments and a 15 min ^{31}P NMR (cycle 2, Figure 5). OGD was induced by switching the normal aCSF to OGD aCSF and the gas from normoxia to hypoxia at the start of the second stacked ^{1}H NMR experiment. OGD aCSF was prebubbled with 95% N_2/5% CO_2 for 30 min to deliver medium without oxygen to the brain slices. During the first 20 min of OGD, the OGD aCSF was dumped to prevent contamination from the remaining oxygenated normal aCSF with glucose, and after that time the medium was recirculated. Depending on the length of the OGD condition (mild: 30 min, moderate: 60 min, severe: 120 min), following cycle 2, the cycle of TEMP - ^{1}H NMR - 15 min ^{31}P NMR - TEMP (cycle 3, Figure 5) was continued until it was time to switch back to the oxygenated normal aCSF (reperfusion time). At this point, another cycle 2 was acquired where media and gases were switched at the beginning of the second stacked ^{1}H NMR scan. Normal aCSF was dumped for the first 20 min of reperfusion and was then recirculated until the end of the experiment. Following the OGD period, cycle 1 was continued for around 4 h after switching back to normoxia conditions until the end of the experiment.

2.7 | ^{1}H and ^{31}P NMR spectroscopy

NMR measurements in the perfusion system were performed using a 600-MHz Bruker Avance III NMR spectrometer with a 10-mm BBO probe. The viability of rat brain slices was assessed by ^{31}P NMR (ns = 600, t = 15 min 17 s or ns = 1200, t = 30 min 22 s; RG = 203). ^{31}P spectra were recorded with power-gated decoupling (zgpg), 64k datapoints, 300 ppm spectral width, and 1 s relaxation delay. To avoid sample heating, ^{1}H was decoupled by weak decoupling pulses (0.21 kHz for nuclear Overhauser effect (NOE) buildup and 0.15 kHz during acquisition) and a WALTZ-16 decoupling sequence. A 70° excitation pulse (Ernst angle) was used for optimal signal sensitivity for the chosen acquisition parameters. Line broadening of 7 Hz was used.

The dynamic changes in metabolites under normoxic and hypoxic conditions were monitored using ^{1}H NMR (ns = 32, t = 2 min 22 s, RG = 114). A one-dimensional (1D) NOESY (noesygppr1d) pulse sequence was applied with presaturation (50 Hz) of water signal during the relaxation delay (1 s) and mixing time (10 ms). A total of 64k datapoints were collected with a spectral width of 16 ppm. The data were processed with 64k real datapoints and line broadening (3 Hz) was applied.

The stacked ^{1}H NMR spectra were recorded as a pseudo two-dimensional NMR experiment, starting a new ^{1}H experiment every 120 s. The acquisition parameters were identical to the 1D NOESY experiment, except the spectral width was increased to 20 ppm.

The distance between DSS and water signals was determined from a pulse-acquire experiment with similar parameters to the 1D NOESY experiment.

Media samples were analyzed using a 600-MHz Bruker Avance III NMR spectrometer dedicated for biofluids (5-mm BBI probe). A 1D NOESY (noesygppr1d) pulse sequence was applied with presaturation (25 Hz) of water signal during the relaxation delay (4 s) and mixing time (10 ms). A total of 64k datapoints were collected with a spectral width of 20 ppm and 32 scans. The data were processed with 128k real datapoints and line broadening (0.3 Hz) was applied.

2.8 | Data analysis

Spectra were analyzed and processed in MestreNova (MestreLab Research, Santiago de Compostela, Spain) using phase correction, multipoint baseline correction, and sum method. Peak Picking based on global spectral deconvolution was used before integrating the peaks of interest and conducting further analysis. Only peaks with an SNR ratio of 3 or higher from both ^{1}H and ^{31}P NMR were included in the further analysis. ^{1}H NMR peaks of interest (Lac, NAA, γ-aminobutyric acid [GABA], Glu, and Cr) were integrated with respect to the DSS peak (integral set to 1, ppm set to 0) in the brain samples spectra. For ^{31}P NMR, the peak of interest (phosphocreatine [PCr]) was integrated with respect to the inorganic phosphate (Pi) peak (integral set to 1, at 2.94 ppm). The mean normalized meabolite levels for each group were plotted versus time from the start of OGD using Excel (Microsoft).

To investigate differences in the recovery of metabolites after the end of OGD and reperfusion with normal aCSF, we also plotted the mean metabolite levels for each group versus time from the start of reperfusion. Student's unpaired two-tailed t-tests were used to test for significant differences between groups at each time point.

2.9 | Analyses of media samples

To correct for metabolite accumulation from recirculating media in the perfused tissue sample, 0.5-ml samples of aCSF were collected from the primary out-line every 30 min during the entire experiment and stored at −20°C until ^{1}H NMR analysis. Samples were thawed and transferred to 5-mm NMR tubes for ^{1}H NMR analysis. The Lac doublet was localized at 1.32 ppm when DSS was set at 0 ppm, while other metabolites were not identified because of the low SNR. Because DSS was used as an internal standard in the media samples as well as in the perfused samples, the metabolite levels in the media could be subtracted from the perfused metabolite levels to determine the metabolite levels of only the brain tissue. To accomplish this, Lac levels from media samples were plotted against collection time. Each OGD experiment was separated into three sections: normoxia, OGD, and reperfusion. Lac levels from the perfused sample in these sections were corrected separately by fitting a linear regression curve to the media Lac levels against time. The contribution of Lac from the media was subtracted from the Lac levels in the perfused sample using the equation from the linear regression curve. The acceptance criteria for applying the correction to the Lac levels were (a) more than three datapoints collected in each section (normoxia, OGD, and reperfusion); and (b) R^2 less than 0.9 (supporting information). All control data were corrected using a single regression curve and the same acceptance criteria.

2.10 | Histology

Brain slices were collected after the perfusion system experiments and were immersion-fixed in formalin (4% formalin aqueous solution). The brain hemisphere that was not used in the perfusion experiments was also immersion-fixed in formalin for comparison. Then brain slices were prepared for tissue processing in the automated wax embedding system, where tissues were dehydrated with a graded series of alcohol concentrations. Samples before the perfusion experiments were thick enough (thickness = 3 mm) to be placed in a tissue cassette without a risk of displacement, but samples after the perfusion experiments were thinner (thickness = 400 μm) and needed extra support in the form of a padding material (supporting information). After the procedure, samples were paraffin-embedded, sectioned (thickness = 4 μm), and stained histologically using hematoxylin–erythrosine–saffron (HES). The stained sections were observed under an optical microscope (x 40, Olympus BX41, Japan) and the results were assessed by a neuropathologist.

3 | RESULTS

3.1 | Metabolic changes in perfused rat brain slices during normoxia and OGD

The ^{31}P NMR spectra were aligned to PCr at −2.52 ppm and the additional metabolites could be detected: Pi (2.94 ppm), α-ATP (−10.11 ppm), γ-ATP (−5.09 ppm), and glycerylphosphorylcholine (GPC) (0.44 ppm), as shown in Figure 6A. The ^{1}H NMR spectra were aligned to DSS at 0 ppm and the following metabolites were detected: Lac (methyl group, 1.32 ppm), NAA (acetyl group, 2.01 ppm), creatine (Cr) (methyl group, 3.02 ppm), GABA (α-methylene group, 2.28 ppm), Glu (γ-methylene group, 2.35 ppm), glucose (anomeric signal [α], 5.2 ppm), and sucrose (anomeric signal) at 5.4 ppm, as shown in Figure 6B.

The PCr and Lac levels in the control group were stable throughout the entire perfusion experiment (Figure 7). In all OGD groups during the OGD period, the levels of PCr and Lac decreased significantly in comparison with the metabolite levels in the control group, with a clear relationship between the length of OGD and decrease in metabolite levels. After switching the media from normal aCSF to OGD aCSF, an absence of

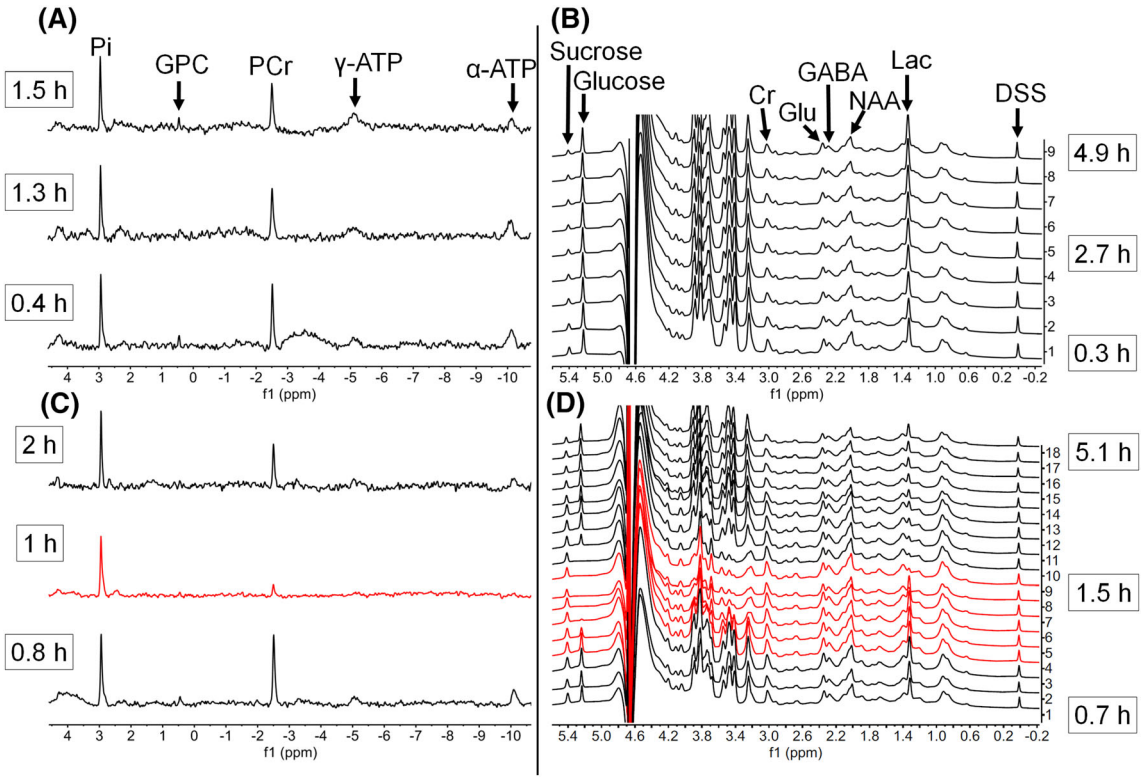

FIGURE 6 Representative ^{31}P and ^{1}H NMR spectra. (A) ^{31}P control, (B) ^{1}H control, (C) ^{31}P oxygen–glucose deprivation (OGD)-30, and (D) ^{1}H OGD-30 acquired from rat brain slices in the perfused artificial cerebrospinal fluid. ^{31}P: three spectra shown for control and OGD experiments. ^{1}H: all acquired spectra are displayed. For both ^{31}P and ^{1}H spectra, the time shown in the black box indicates the duration from when the perfusion system was placed into the magnet. The OGD period is marked in red

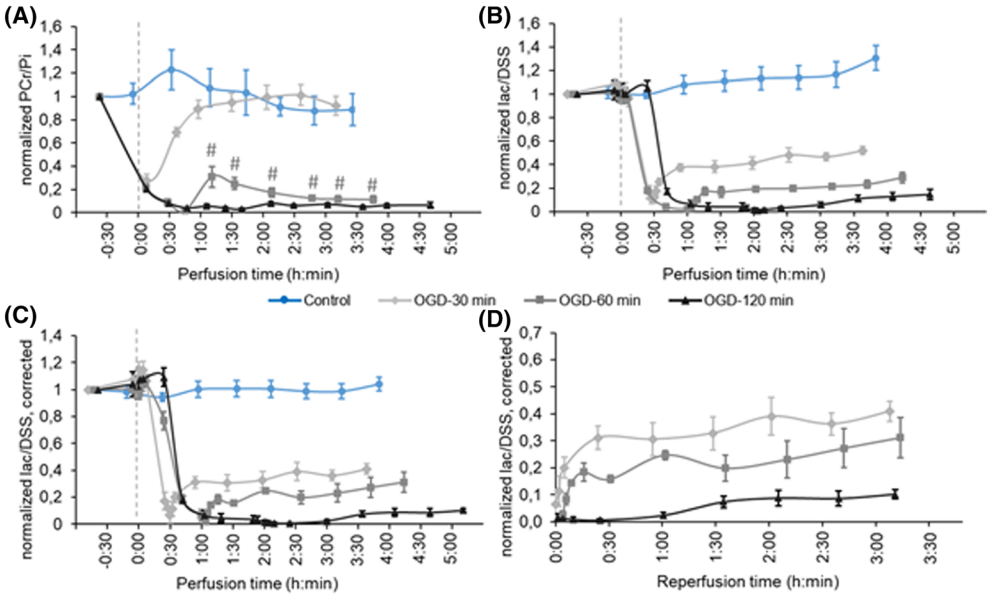

FIGURE 7 ^{1}H NMR and ^{31}P NMR signal intensities from perfused rat brain slices during normoxia (control), and oxygen–glucose deprivation (OGD)-30, -60, and -120 min. OGD starts at time 00:00 (dashed line). (A) Phosphocreatine (PCr) integrated to inorganic phosphate (Pi) peak relative to the first ^{31}P NMR spectrum. (B) Lactate (Lac)/sodium trimethylsilylpropanesulfonate (DSS) relative to the first ^{1}H NMR spectrum before correcting for recirculating Lac. (C) Lac/DSS relative to the first ^{1}H NMR spectrum after Lac correction. (D) Data from (C) plotted with the x-axis showing the time from the start of reperfusion to allow a comparison of trends in Lac concentration after reperfusion between groups. Data shown are mean ± SEM. Note that the six last datapoints in the two perfusion experiments are not included in the ^{31}P NMR data results because of overlapping peaks in the spectra (supporting information)

glucose (5.4 ppm, Figure 6D) was seen in ^{1}H NMR spectra, confirming that the sample was exposed to OGD conditions. Figure 7A shows that PCr levels dropped to almost zero in both the OGD-60 and -120 groups before reperfusion with normal aCSF. After reperfusion with normal aCSF, levels of PCr increased in the OGD-30 and -60 groups but not in the -120 group. However, while PCr levels returned to pre-OGD levels in the OGD 30-min group, PCr levels in the OGD-60 group dropped again in the hours following the initial increase after reperfusion and remained at a similarly low level as OGD-120 for the remainder of the experiment. Figure 7B shows that there was a steady increase in Lac levels after reperfusion in all OGD groups for the duration of the experiment. While none of the groups reached their pre-OGD levels, there was a clear relationship between Lac levels and duration of OGD, with OGD-30 and -120 ending highest and lowest, respectively. A complete report of metabolite levels during the reperfusion time is provided in the supporting information.

The aCSF media were recirculated during normoxia prior to OGD. Once the aCSF media were switched to OGD buffer, media were dumped for the first 20 min, then recirculated. Similarly, media were dumped for the first 20 min after switching back to normoxia media, then recirculated. A steady increase of Lac levels over time was observed in every experimental group (Figure 7B). Because metabolites removed from the perfused brain by the media would be reintroduced into the NMR tube during recirculation of the media, the metabolite measurement would be a sum of the brain concentration and media concentration. To be able to estimate the contribution from only the Lac in the brain sample located in the NMR active region, we decided to correct the measured Lac levels by substracting the contribution from recirculating Lac in the aCSF (Figure 7C). Following the correction, we observed a small decrease of Lac in brain tissue in every experiment, as well as smaller SEM of Lac in the control group (Figure 7C).

NAA, Glu, GABA, and Cr levels in the control groups were stable throughout the entire perfusion experiment (Figure 8). NAA levels in the OGD groups slightly decreased over time after the start of the OGD, with the largest decrease in the OGD-120 group (Figure 8A). Levels of Glu decreased significantly when compared with the metabolite levels in the control group, with a dependency on the length of the OGD; the longer the OGD, the larger the decrease of Glu levels (Figure 8B). GABA levels increased compared with the levels in the control group, with the smallest increase in the OGD-30 group (Figure 8C). Cr levels decreased slightly over time compared with the stable metabolite levels in the control group (Figure 8D).

When comparing metabolite levels between the different OGD groups after reperfusion with normal aCSF, OGD-30 had higher Glu levels than OGD-120 at all time points, with OGD-60 having levels in between (Figure S5 and Table 1). NAA and Cr levels in the OGD-30 and -60 groups were similar to controls, with OGD-120 having lower levels during the first 60–90 min after the start of reperfusion. Therafter, NAA and Cr levels in OGD-30 and -60 decreased, with OGD-60 displaying a more steep drop than OGD-30. Although a parallel decrease in NAA and Cr levels was seen in the OGD-120 group, the differences between the OGD groups were reduced over time. For GABA, there was a tendency towards levels in the OGD-30 group to become more similar to controls over time, while they remained elevated in the OGD-60 and -120 groups (Figure S5 and Table 1).

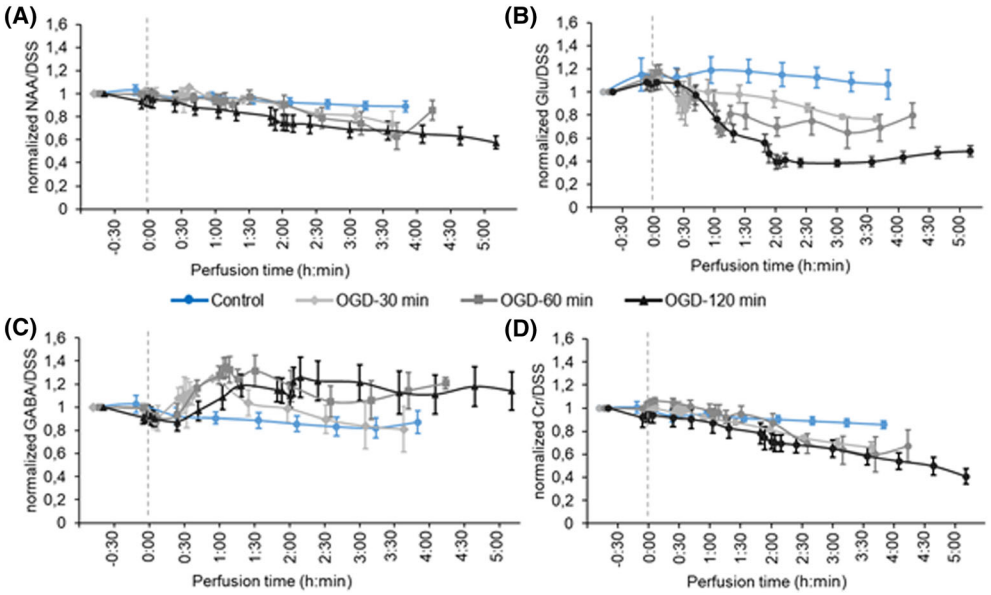

FIGURE 8 ^{1}H NMR signal intensities from perfused rat brain slices during normoxia (control) and oxygen–glucose deprivation (OGD-30, -60, -120 min) that starts at time 00:00 (dashed line). (A) N-acetylaspartic acid (NAA) integrated to sodium trimethylsilylpropanesulfonate (DSS) peak relative to the first ^{1}H NMR spectrum. (B) Glutamate (Glu)/DSS relative to the first ^{1}H NMR spectrum. (C) γ-aminobutyric acid (GABA)/DSS relative to the first ^{1}H NMR spectrum. (D) Creatine (Cr)/DSS relative to the first ^{1}H NMR spectrum. Data shown are mean ± SEM

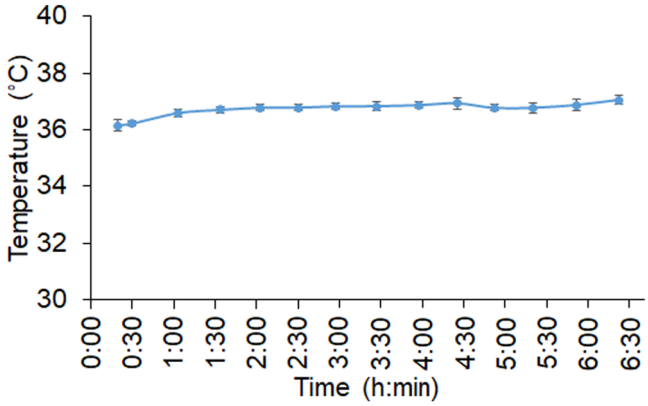

FIGURE 9 Temperature (mean ± SEM, n = 22) of the perfused tissue sample in the spectrometer bore over time during the control and oxygen–glucose deprivation (OGD) experiments

3.2 | Temperature and oxygen levels

The temperature of the perfused aCSF sample in the spectrometer bore was measured after each ^{31}P NMR applied. Figure 9 shows that the temperature was kept stable at 36.7 ± 0.1°C (mean ± SEM) in the control and OGD groups during the entire experiment.

3.3 | Media samples analysis

^{1}H NMR of the aCSF samples collected from the primary out-line showed an increased level of Lac over time in both the control and OGD groups. Media samples collected from the OGD period were too few (n ≤ 2) to properly correct Lac levels during that time. Lac levels were corrected in all of the experiments in the control group, one experiment in the OGD-60 group was not corrected due to failure in meeting the requirements, and three experiments in the OGD-30 group were corrected either only in the section before or after the OGD period.

3.4 | Histology

HES staining of the brain tissue before the perfusion experiments showed no morphological changes in the matrix of the tissue as well as no brain cell damage (Figure 10A).

Brain slices in the control, OGD-30, -60, and -120 groups (Figure 10B,C,D,E, respectively) collected after the perfusion experiments showed no morphological changes of brain cells, but a visible wash-out effect of the extracellular matrix. No significant changes between these groups were observed. However, compared with the thicker brain tissue before the perfusion experiments, we observed a high amount of vacuolization of the neuropil in all the groups after the perfusion experiments (examples are indicated with arrows in Figure 10B–E). This is a common reproducible histological artefact seen in rodent brains attributed to prolonged holding of fixed tissue in 70% alcohol within an enclosed system automatic tissue processor.[16]

4 | DISCUSSION

The aim of this study was to establish an HI brain injury model using brain slices perfused in an NMR-compatible perfusion system with a stable and controlled environment.

The first important step was to establish a perfusion system that kept the tissue at a stable and physiological temperature inside the spectrometer bore. One challenge that we encountered in that respect was the significant loss of temperature between the aCSF reservoir placed in the water bath and the perfused aCSF sample in the NMR tube. We managed to solve this by increasing the temperature of the water bath and by minimizing heat loss along the in-line by installing a 1.5-m long water-heated tube set at 60°C surrounding the in-line and primary out-line. To have absolute control of the temperature in the perfused sample in the spectrometer bore, an established NMR thermometer method[15] using an NMR sample that has a known temperature-dependent chemical shift difference over the temperature range of 282–330 K was used.

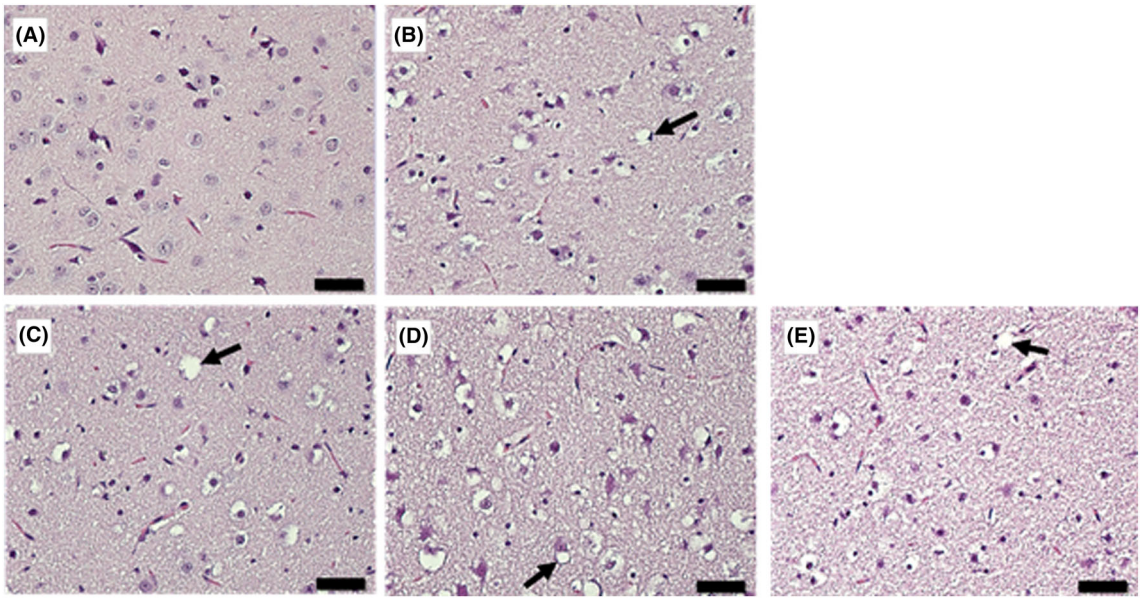

FIGURE 10 Rat brain slices before and after perfusion experiments stained with hematoxylin–eosin–saffron (HES) (images at x 40, scale bar = 100 μm). (A) Before the perfusion experiment. After the perfusion experiment in the (B) Control, and (C) Oxygen–glucose deprivation (OGD)-30, (D) -60, and (E) -120 groups

In our study, DSS was added as an internal standard to the aCSF. We measured the chemical shift difference between the H_2O and DSS peaks from the aCSF sample and found that the probe temperature was linear over the temperature range of 310–312 K. This method allowed for a quick and easy probe temperature adjustment to 37°C, when needed. The equation for the sample temperature calculation fit the data very well with a correlation coefficient $R^2 = 0.99$. However, in future studies, the linear relationship between the chemical shift difference of the H_2O and DSS peaks and temperature should be tested over a wider temperature range, especially when including hypothermia treatment after OGD. If linearity is compromised, the relationship could be estimated by a higher order polynomial function. Measuring the temperature from the NAA – H_2O ^1H NMR frequency distances provided similar accuracy, but reduced precision (data not shown), due to difficulties in determining the NAA peak center in some spectra. Besides the H_2O-DSS method, an alternative solution to measure the sample temperature during experiments that could be explored would be by using a fiber optic temperature sensor that is compatible with NMR.

Another important environmental feature to control inside the perfusion system is oxygenation. In most of the studies using OGD models with brain slices, the aCSF is prebubbled with a gas mixture of 95% O_2/5% CO_2 for 30–45 min before its use[8,17] to fully saturate the medium with oxygen. Using an oxygen macrosensor, the time required to reach oxygen levels from its minimum to maximum in the perfused aCSF sample was measured. Unfortunately, the oxygen macrosensor is not NMR-compatible, so it was not possible to measure the oxygen content in the perfused aCSF sample while located in the spectrometer bore. Therefore, oxygenation calibration experiments were carried out using an identical perfusion system but with the sample outside the spectrometer in a heat bath set to 37°C. Maximum (83% O_2) and minimum (10.5% O_2) oxygenation levels of the buffer were measured 25 min after switching gases. The discrepancy between applied (maximum 95% and minimum 0%) and measured (maximum 83% and minimum 10.5%) buffer oxygenation can be explained by the characteristics of gas solubility in liquids. The solubility of oxygen in water decreases with increasing temperature and increasing salinity,[18] which in our case of using an aCSF with a high content of dissolved salts and temperature of 37°C, could explain the lower measured value at maximum oxygenation. In addition, even although our system was established to be leakage-free for fluids, it includes many connectors between tubes, and it is not created with a vacuum. A not completely air-tight system could allow exchange of the applied oxygen in the perfusion system with the room air, thus preventing the oxygen levels in the system from reaching the extreme low and high limits (0% and 95%, respectively). When the oxygen consumption in the sample is the aim of the study, an NMR-compatible oxygen sensor could be used to continuously measure the O_2 levels in the sample.

The next step in an optimal perfusion system with the OGD model was a smooth switch from normoxic to hypoxic conditions, as well as a simultaneous change from the glucose- to the glucose-free medium. In an ideal situation, all of the perfusion system media would have been dumped after a first pass through the NMR tube, to remove any recirculation effects. Unfortunately, the costs of using 10% of D_2O in the aCSF were considered to be too high. The volume of tubing used in the perfusion system was calculated and, knowing the buffer flow rate, the minimal time to completely change the buffers from normal to OGD was measured. We decided to dump the media for 20 min after a switch to another buffer, which was five times longer than the time of complete aCSF filling in the perfusion system. After this time, the aCSF was recirculated. Recirculating the media caused a steady increase in metabolite levels over time (in the control and OGD groups), especially Lac, which was probably

washed from the brain tissue and released into the aCSF. To correct for this and estimate the metabolite levels from the brain tissue only, aCSF samples were collected from the primary out-line every 30 min during each experiment. Lac levels in the buffer were plotted as a function of time before and after the OGD period. For datasets containing at least three datapoints, Lac levels were fitted with a linear regression curve and each perfusion experiment was corrected separately. Corrections were applied to Lac data where the regression line fitted the data well (correlation coefficient $R^2 > 0.90$). Because samples were collected every 30 min, there were generally too few aCSF samples collected during the OGD period to perform a Lac level correction. However, Lac levels measured in the aCSF collected during the OGD period in all OGD groups were close to 0. In addition, the uncorrected metabolite levels decreased significantly upon switching to OGD and almost reached 0, as well as when compared with the starting levels. This reduction in metabolite level can be explained by a wash-out of recirculating metabolites associated with the switch to the new OGD aCSF.

The pattern of the Lac levels was similar before and after applied corrections. We believe that the main conclusion of the study was not affected by applying a Lac correction for the presence of recirculating Lac. Nevertheless, it is interesting and useful to measure the actual tissue metabolite levels as accurately as possible. In the future, an improvement to the experimental method could be to collect aCSF samples more frequently during the OGD period, or by using an external deuterated solvent as a lock reference, allowing the media to be dumped throughout the entire experiment.

The biggest advantage of using brain slices in the OGD model instead of neuronal cell cultures is that the tissue morphology is relatively unchanged from the intact animal structure because intercellular connections are preserved.[9] However, when preparing brain slices, the tissue is exposed to tissue trauma and periods when glucose and oxygen supply to the tissue are absent, especially between the decapitation and extraction of the brain and when cutting slices. In all perfusion experiments, this time has been kept as short and as similar as possible so that the potential damage to the tissue would be comparable (data not shown). In addition, a slicing aCSF (rich in sucrose and magnesium, poor in calcium) was used to immerse brain tissue after decapitation and before slicing, to prevent brain edema and neuronal injury due to the slice-preparation process.[19]

Previous studies using in vivo models of HI in neonatal rats have shown differences between males and females when it comes to effects on the brain after HI, suggesting that males are more adversely affected by HI injury relative to comparably injured females.[20,21] To avoid sex as a possible confounding factor, we therefore aimed to only use female rats in our study. However, some of the initial experiments included male rats and, after careful consideration, we decided to include them in our study (one male in the control group and one in the OGD-120 group). This decision was based upon analysis of the data collected from the perfusion experiments showing no differences in metabolite levels within the OGD-120 group and within the control group between males and females.

In this study, we used MestreLab software for ^{1}H and ^{31}P NMR spectral analysis. The software provided useful tools to correct the challenging baseline in the ^{31}P NMR spectra. Furthermore, partially overlapping signals were separated using deconvolution to distinguish the contributions from individual peaks. Even although all spectra were processed in the same way, a further improvement could be to use a more automated approach, applying software that utilizes predefined parameters like chemical shift, coupling constants, linewidth, and signal intensity for each metabolite signal of interest.

As expected, ^{1}H and ^{31}P NMR spectra in our study showed that the Lac and PCr levels depend on the length of the OGD period and are significantly different when compared with the levels of metabolites in the control group. In our study, Lac in the rat brain slices during and after OGD was decreased compared with the control group. A similar effect was seen in a study of OGD in adult rat brain slices conducted by Thomaz et al.,[22] where an ischemic event led to a decrease in Lac and ATP in hippocampal slices.

An important finding in our study was the relationship between OGD length and the trajectory of recovery of brain metabolites after OGD. The greatest recovery to pre-OGD levels was seen in the shortest OGD group. Taking control levels as 100%, the Lac after the OGD period recovered to 64% ± 9% for OGD-30, 41% ± 10% for OGD-60, and 19% ± 3% for OGD-120. These results show how the model set-up can be used to monitor the recovery of energy metabolism in the brain tissue after OGD, which is a significant factor for brain tissue survival.[23] Together with the high reproducibility of different levels of injury, it shows the potential of the model set-up for future studies of the influence of potential treatment on energy recovery after brain HI.

Our study measured the changes in the brain tissue 3–4 h after the end of the OGD period. Lac levels in the OGD-30 group did not recover completely after the OGD period, presumably because this required more time. However, there was an increasing trend of Lac levels over time in the OGD-30 group, while the levels of Lac in OGD-60 and -120 were more stable and lower. Moreover, during this study we did not observe above normal Lac levels or a new reduction in PCr, which are typically observed clinically during a secondary energy failure that usually occurs 8–24 h after HI brain injury.[24] A longer experiment could be relevant for investigations into a secondary energy failure post-OGD in our model.

In contrast to our ^{1}H NMR results, a study using extracts of neonatal rat brain slices showed no change of Lac levels measured by ^{1}H NMR in samples at the end of recovery after 45 min of OGD in comparison with initial Lac levels.[25] The differences between this and our study are the absence of sucrose in the OGD aCSF medium, slower media flow (3 ml/min compared with 5 ml/min in our study), and perchloric acid extraction of brain slices taken out from the perfused chamber instead of measuring the metabolite levels of the perfused brain slices directly by NMR. A different study using adult rat brain slices reported an increase in the ratio of Lac to NAA after 20 min of ischemia compared with the initial levels of metabolites.[26] The opposite trend in Lac to NAA response could be explained by the stop-flow method used in this study, leading to an

accumulation of Lac due to increased production from the anaerobic respiration and no removal by flow, as opposed to the continuous flow technique used in our experimental set-up. Another, but less expected, explanation for the differences observed in the Lac is the possible inhibitory effect of sucrose from the OGD aCSF on Lac production. However, the literature reports several brain-slice studies[27–29] employing similar protocols to ours, where glucose in the aCSF medium is replaced with sucrose in the OGD medium to maintain osmolarity of the buffer, and no inhibitory effect of sucrose on Lac production was reported.

NAA levels slightly decreased over time and might indicate the loss of neurons in the brain tissue after applied OGD, a situation that is also observed in patients after HI.[30] A similar trend was observed with the levels of Cr, where Cr is the marker of energy in the tissue, thus its decrease indicates a loss of energy in the brain slices after depriving the brain tissue of oxygen. The increased GABA and Glu levels can be related to their function as neurotransmitters and ongoing excitotoxicity in the reperfusion phase. Another explanation of decreasing levels of metabolites could be the movement of the brain tissue from the active region over time due to the continuous perfusion of the sample. The importance of using a suitable filter material and robust mounting technique is crucial to prevent sample movement and avoid pressure build-up within the NMR tube. In addition, the position of sample components in the NMR tube should be inspected at the end of the bioreactor experiment.

Histological analysis of brain slices before and after perfusion experiments was carried out using HES staining. We observed a wash-out effect of the extracellular matrix in the brain tissue that had been in the perfusion system in comparison with the sample before the perfusion experiment. This observation was probably a result of continuous perfusion of the 400-μm slices for 5–6 h in the perfusion system. In addition, extensive vacuolization of the neuropil was only seen after perfusion experiments and occurred to a similar extent in all control and OGD groups. This was probably caused by inefficient dehydration of the tissue during the fixation process, which is a common occurrence observed in samples from the rodent nervous system.[16] Moreover, perfused samples underwent a different histology preparation process due to their thin and fragile state and required the use of a tissue cassette with extra padding material to prevent displacement of the thin brain slices. This procedure could have influenced the quality of the fixation, causing these artifacts. In addition, no neuronal damage typically associated with HI in brain tissue was seen in any of the groups. The pathogenic mechanisms of HI injury evolve over time; neuronal death and the associated morphologic changes can be delayed for several days.[31] Therefore, it is likely that it was too early to see morphological neuronal damage caused by the lack of oxygen and glucose 3–4 h after the end of the OGD in our study. To see the changes made by the OGD in the brain tissue, experiments lasting longer than 12–24 h would be more suitable.

Brain slices in the perfusion system and OGD model can be used for studying pathophysiological changes in adult stroke or neonatal hypoxic–ischemic brain injury.[9] Although there are differences between neonatal and adult brains, the basic response to OGD remained the same in a study conducted by Espanol et al.[26] using adult rat brain slices, and in a study performed by Liu et al.[32] using slice extracts from 7-day-old rat pups. This supports the relevance of also using this model system for neonatal HI studies. In these studies, a decrease of PCr and ATP levels was observed after OGD was applied; a similar effect was seen in our perfusion set-up, followed by recovery of the metabolite levels measured by NMR. However, many in vivo studies show that the brains of immature animals are more resistant to oxygen deprivation than the brains of adult animals,[33,34] so optimization of the OGD duration should be carried out for a neonatal brain set-up of the perfusion system. Another limitation of the perfusion system for the purpose of studying neonatal HI is that it is only feasible to process one rat brain per day, resulting in making the choice of either using one pup at the same age from many litters or using more pups from one litter, but with a wider range of ages.

Furthermore, using the perfusion system to mimic adult stroke would ideally include stopping the flow of the medium. Because the model system is not air-tight, it would be difficult to generate very low oxygen concentrations owing to gas exchange with the air surrounding the perfusion medium, thus limiting the versatility of the set-up.

Despite its limitations, this ex vivo system permits direct treatment with pharmacological agents, which provide surrogate therapeutic screening without recourse to whole animal studies. The possibility to accurately control and monitor the temperature of the sample while inside the NMR spectrometer also allows for studies of therapeutic hypothermia in combination with neuroprotective agents.

5 | CONCLUSION

We successfully developed an NMR-compatible perfusion system that allowed reproducible metabolic characterization of three different severity levels of OGD in rat brain tissue, mimicking hypoxic–ischemic brain injury. We were able to maintain the viability of rat brain slices for more than 5 h under controlled perfusion conditions designed to ensure adequate oxygen and nutrient supply, as well as a stable physiological temperature of 37°C. ^{31}P NMR provided satisfactory spectral quality to observe changes in energy metabolism of brain tissue. ^{1}H NMR showed changes in key metabolites after applied OGD that can be used to evaluate tissue injury severity. The perfusion system will be suitable for future studies to characterize the impact of therapeutic agents on tissue energy metabolism recovery after OGD.

ACKNOWLEDGMENTS

MR and animal studies were performed at the MR Core Facility and Comparative Medicine Core Facility, and histology studies were performed at the Cellular and Molecular Core Facility at the Norwegian University of Science and Technology. Special thanks to Knut Sverre Grøn for technical

support at CoMed. Special thanks to Ingunn Nervik for expertise and advice with histological methods, and Sverre Helge Torp for the help with histological analysis. We would also like to thank Arnfinn Sira for making custom-made adapters used to connect the perfusion lines inside the water-heated tube in the perfusion system. Thanks to Chaumeil, Kurhanewicz, and Ronen labs, University of California in San Francisco (UCSF, USA) for help with perfusion set-up design and problem solving. Thanks to Katz-Brull lab (Hebrew University Faculty of Medicine, Israel) for useful discussions about the perfusion set-up. The authors declare no competing interests. This work was financially supported by the Faculty of Medicine and Health Sciences at the Norwegian University of Science and Technology (AM: PhD stipend).

ORCID

Deborah K. Hill https://orcid.org/0000-0002-6441-5489
Trygve Andreassen https://orcid.org/0000-0001-5295-5501
Marius Widerøe https://orcid.org/0000-0002-0830-7555

REFERENCES

1. Lacerte M, Shapshak AH, Mesfin FB. Hypoxic brain injury. *CPD Anaesth.* 2021;9(3):157-159.
2. Evans MRB, White P, Cowley P, Werring DJ. Revolution in acute ischaemic stroke care: a practical guide to mechanical thrombectomy. *Pract Neurol.* 2017;17(4):252-265. doi:10.1136/PRACTNEUROL-2017-001685
3. Melkonian EA & Schury MP Biochemistry, Anaerobic Glycolysis. Stat Pearls Publishing; 2021. https://www.ncbi.nlm.nih.gov/books/NBK546695/. Accessed September 25, 2021.
4. McLean C, Ferriero D. Mechanisms of hypoxic-ischemic injury in the term infant. *Semin Perinatol.* 2004;28(6):425-432. doi:10.1053/J.SEMPERI.2004.10.005
5. Rumajogee P, Bregman T, Miller SP, Yager JY, Fehlings MG. Rodent hypoxia-ischemia models for cerebral palsy research: a systematic review. *Front Neurol.* 2016;7(57). doi:10.3389/fneur.2016.00057
6. Sommer CJ. Ischemic stroke: experimental models and reality. *Acta Neuropathol.* 2017;133(2):245-261. doi:10.1007/s00401-017-1667-0
7. Gmati D, Chen J, Jolicoeur M. Development of a small-scale bioreactor: Application to in vivo NMR measurement. *Biotechnol Bioeng.* 2005;89(2):138-147. doi:10.1002/bit.20293
8. Fernández-López D, Martínez-Orgado J, Casanova I, et al. Immature rat brain slices exposed to oxygen–glucose deprivation as an in vitro model of neonatal hypoxic–ischemic encephalopathy. *J Neurosci Methods.* 2005;145(1–2):205-212. doi:10.1016/J.JNEUMETH.2005.01.005
9. Cho S, Wood A, Bowlby M. Brain slices as models for neurodegenerative disease and screening platforms to identify novel therapeutics. *Curr Neuropharmacol.* 2007;5(1):19-33. doi:10.2174/157015907780077105
10. Cimarosti H, Henley JM. Investigating the mechanisms underlying neuronal death in ischemia using in vitro oxygen-glucose deprivation: potential involvement of protein SUMOylation. *Neuroscientist.* 2008;14(6):626-636. doi:10.1177/1073858408322677
11. Russell WMS, Burch RL. The Principles of Humane Experimental Technique. *Med J Aust*. 1960;1:500-500. https://doi.org/10.5694/j.1326-5377.1960.tb73127.x
12. Shaul D, Grieb B, Sapir G, et al. The metabolic representation of ischemia in rat brain slices: A hyperpolarized 13 C magnetic resonance study. *NMR Biomed.* 2021;34:e4509. 10.1002/nbm.4509
13. Opitz-Araya X, Barria A. Organotypic hippocampal slice cultures. *J Vis Exp.* 2011;48:2462. doi:10.3791/2462
14. Corbett RJT, Laptook AR, Tollefsbol G, Kim B. Validation of a noninvasive method to measure brain temperature in vivo using 1H NMR spectroscopy. *J Neurochem.* 1995;64(3):1224-1230. doi:10.1046/J.1471-4159.1995.64031224.X
15. Findeisen M, Brand T, Berger S. A 1H-NMR thermometer suitable for cryoprobes. *Magn Reson Chem.* 2007;45(2):175-178. doi:10.1002/mrc.1941
16. Wells GAH, Wells M. Neuropil vacuolation in brain: a reproducible histological processing artefact. *J Comp Pathol.* 1989;101(4):355-362. doi:10.1016/0021-9975(89)90018-2
17. Patiño P, Parada E, Farré-Alins V, et al. Melatonin protects against oxygen and glucose deprivation by decreasing extracellular glutamate and Nox-derived ROS in rat hippocampal slices. *Neurotoxicology.* 2016;57:61-68. doi:10.1016/J.NEURO.2016.09.002
18. Lange R, Staaland H, Mostad A. The effect of salinity and temperature on solubility of oxygen and respiratory rate in oxygen-dependent marine invertebrates. *J Exp Mar Biol Ecol.* 1972;9(3):217-229. doi:10.1016/0022-0981(72)90034-2
19. Ting JT, Daigle TL, Chen Q, Feng G. Acute brain slice methods for adult and aging animals: application of targeted patch clamp analysis and optogenetics. *Methods Mol Biol.* 2014;1183:221-242. doi:10.1007/978-1-4939-1096-0_14
20. Smith AL, Garbus H, Rosenkrantz TS, Fitch RH. Sex differences in behavioral outcomes following temperature modulation during induced neonatal hypoxic ischemic injury in rats. *Brain Sci.* 2015;5(2):220-240. doi:10.3390/brainsci5020220
21. Hill CA, Threlkeld SW, Fitch RH. Early testosterone modulated sex differences in behavioral outcome following neonatal hypoxia ischemia in rats. *Int J Dev Neurosci.* 2011;29(4):381-388. doi:10.1016/j.ijdevneu.2011.03.005
22. Thomaz DT, Rafognatto R, Luisa A, et al. Guanosine neuroprotective action in hippocampal slices subjected to oxygen and glucose deprivation restores ATP levels, lactate release and glutamate uptake impairment: involvement of nitric oxide. *Neurochem Res.* 2020;45(9):2217-2229. doi:10.1007/s11064-020-03083-2
23. Magistretti PJ, Allaman I. A cellular perspective on brain energy metabolism and functional imaging. *Neuron.* 2015;86(4):883-901. doi:10.1016/j.neuron.2015.03.035
24. Hanrahan JD, Cox IJ, Azzopardi D, et al. Relation between proton magnetic resonance spectroscopy within 18 hours of birth asphyxia and neurodevelopment at 1 year of age. *Dev Med Child Neurol.* 1999;41(2):76-82. doi:10.1017/S0012162299000171
25. Liu J, Litt L, Segal MR, Kelly MJS, Yoshihara HAI, James TL. Outcome-related metabolomic patterns from 1H/31P NMR after mild hypothermia treatments of oxygen—glucose deprivation in a neonatal brain slice model of asphyxia. *J Cereb Blood Flow Metab.* 2010;31(2):547-559. doi:10.1038/jcbfm.2010.125

26. Espanol MT, Litt L, Chang L-H, James TL, Weinstein PR, Chan PH. Adult rat brain-slice preparation for nuclear magnetic resonance spectroscopy studies of hypoxia. *Anesthesiology*. 1996;84(1):201-210. doi:10.1097/00000542-199601000-00022
27. Meyer DA, Torres-altoro MI, Tan Z, et al. Ischemic stroke injury is mediated by aberrant Cdk5. *J Neurosci*. 2014;34(24):8259-8267. doi:10.1523/JNEUROSCI.4368-13.2014
28. Murata A, Agematsu K, Korotcova L, Gallo V, Jonas RA, Ishibashi N. Rodent brain slice model for the study of white matter injury. *J Thorac Cardiovasc Surg*. 2013;146(6):1526-1533. doi:10.1016/j.jtcvs.2013.02.071
29. Juzekaeva E, Gainutdinov A, Mukhtarov M, Khazipov R. Dynamics of the hypoxia-induced tissue edema in the rat barrel cortex in vitro. *Front Cell Neurosci*. 2018;12:502 doi:10.3389/fncel.2018.00502
30. Robertson NJ, Cox IJ, Cowan FM, Counsell SJ, Azzopardi D, Edwards AD. Cerebral intracellular lactic alkalosis persisting months after neonatal encephalopathy measured by magnetic resonance spectroscopy. *Pediatr Res*. 1999;46(3):287-296. doi:10.1203/00006450-199909000-00007
31. Rahaman P, Del Bigio MR. Histology of brain trauma and hypoxia-ischemia. *Acad Forensic Pathol*. 2018;8(3):539-554. doi:10.1177/1925362118797728
32. Liu J, Litt L, Segal MR, Kelly MJS, Yoshihara HAI, James TL. Outcome-related metabolomic patterns from H/31 P NMR after mild hypothermia treatments of oxygen – glucose deprivation in a neonatal brain slice model of asphyxia. *J Cereb Blood Flow Metab*. 2011;31(2) 2011:547-559. doi:10.1038/jcbfm.2010.125
33. Fazekas JF, Alexander FAD, Himwich HE. Tolerance of the newborn anoxia. *Am J Physiol*. 1941;134(2):281-287. doi:10.1152/AJPLEGACY.1941.134.2.281
34. Rice JE, Vannucci RC, Brierley JB. The influence of immaturity on hypoxic-ischemic brain damage in the rat. *Ann Neurol*. 1981;9(2):131-141. doi:10.1002/ana.410090206

SUPPORTING INFORMATION

Additional supporting information may be found in the online version of the article at the publisher's website.

How to cite this article: Molska A, Hill DK, Andreassen T, Widerøe M. Perfusion system for studying dynamic metabolomics in rat brain slices exposed to oxygen–glucose deprivation using proton and phosphorus nuclear magnetic resonance. *NMR in Biomedicine*. 2022; e4703. doi:10.1002/nbm.4703